

## Systematics of optimum $Q$ values in multinucleon transfer reactions induced by heavy ions

T. Mikumo,\* I. Kohnno, K. Katori,\* T. Motobayashi,† S. Nakajima, M. Yoshie,\* and H. Kamitsubo

*Institute of Physical and Chemical Research, Wako-shi, Saitama, Japan*

(Received 15 April 1976)

The most probable effective  $Q$  values,  $Q_{\text{eff}}^m$ , for multinucleon transfer reactions  $A(a, b)B$  ( $M_b < M_a$ ) have been systematically studied on  $fp$ -shell nuclei and Zr-Mo isotopes induced by  $^{14}\text{N}$  and  $^{12}\text{C}$ , in the energy range between 60 and 100 MeV. As regards the "quasielastic" part of the bump in the energy spectrum, the dependence of  $Q_{\text{eff}}^m$  on the incident and outgoing channel variables, i.e.,  $A$ ,  $a$ ,  $E_i$ ,  $\theta$ , and  $n$ , the number of transferred nucleons, has been extensively investigated. The present data, together with those obtained at higher energies by the Dubna group, show systematic behaviors of  $Q_{\text{eff}}^m$ : (i) for a given  $A(a, b)B$  and  $E_i$ ,  $Q_{\text{eff}}^m$  changes little with  $\theta_{\text{lab}}$ , (ii) at a given  $E_i$ ,  $Q_{\text{eff}}^m$  of  $(a, b)$  is nearly the same for adjacent  $A$  and is not sensitive to their individual nuclear structure, and (iii) the linear relation  $Q_{\text{eff}}^m = \alpha_{\text{eff}} n + \beta_{\text{eff}}$  holds for  $n \leq 4-5$ , whereas the linearity breaks down for larger  $n$ . The relation  $\alpha_{\text{eff}} = -0.1 (E_i - V_i) - 0.9$  MeV holds for a wide range of reactions. The ratio of the most probable effective velocity to the incident velocity  $v_f^m/v_i$  at the transfer region decreases from about unity to 0.4–0.5 as  $n$  increases. The differences in reaction mechanisms for smaller  $n$  and larger  $n$  have been discussed.

[ NUCLEAR REACTIONS  $^{52,53}\text{Cr}(^{14}\text{N}, x)$ ,  $x = ^{13,12}\text{C}$ ,  $^{12,11,10}\text{B}$ ,  $^{10,9,7}\text{Be}$ ,  $^7,6\text{Li}$ ,  $^4\text{He}$ ;  $E = 64, 70, 80, 90, 95$  MeV,  $\theta = 10-33^\circ$ ;  $^{90}\text{Zr}(^{14}\text{N}; ^{13,12}\text{C}, ^{11}\text{B})$ ,  $E = 75$  MeV,  $\theta = 30.5^\circ$ ;  $^4\text{Mo}(^{14}\text{N}, x)$ ,  $A = 92, 94, 95, 96, 97, 98, 100$ ,  $E = 97$  MeV,  $x = ^{13,12}\text{C}$ ,  $^{12,11,10}\text{B}$ ,  $^{10,9,7}\text{Be}$ ,  $^7,6\text{Li}$ ,  $^4\text{He}$ ,  $\theta = 25, 30^\circ$ ;  $^{92}\text{Mo}(^{12}\text{C}; x)$ ,  $x = ^{10}\text{B}$ ,  $^{10,9,7}\text{Be}$ ,  $^7,6\text{Li}$ ,  $E = 90$  MeV,  $\theta = 20^\circ$ ;  
measured energy spectra of  $x$  and optimum  $Q$  values. ]

### I. INTRODUCTION

In multinucleon transfer reactions  $A(a, b)B$  induced by heavy ions at energy much higher than the Coulomb barrier, the shape of the spectrum of the reaction products is mainly characterized by a continuous bell-shaped form (bump). The systematics of the most probable or optimum  $Q$  values,  $Q^m$ , of the reactions, and their dependence on the incident and exit channel variables have been one of the main subjects in the investigation of multinucleon transfer reactions with heavy ions from a macroscopic point of view.<sup>1-3</sup>

For sub-Coulomb reactions, the behavior of  $Q^m$  has been explained by models assuming Rutherford trajectories for the scattering particles. Somewhat different assumptions lead to different "optimum"  $Q$  values.<sup>4-6</sup>

For reactions in an energy region well above the Coulomb barrier, several different models have been proposed<sup>7-9</sup> to reproduce the experimental  $Q^m$  values, which are as yet limited to reactions at fairly high bombarding energies and/or to very heavy target nuclei.<sup>1</sup> The models proposed in Refs. 7-9 have been able to fit the available data, but the implications of these models are somewhat contradictory. Wilczyński,<sup>9</sup> for instance, claims that  $Q^m$  is determined mainly by the mass balance of the nuclei involved in the reaction; Siemens *et al.*<sup>8</sup> point out the essential

role of recoil effects and a strong dependence on reaction kinematics, while Brink<sup>7</sup> suggests that the key factor determining  $Q^m$  or the most probable "effective"  $Q$  values,  $Q_{\text{eff}}^m$  (see Sec. III), is the velocity of the scattering particles.

In an earlier survey of the systematics of  $Q^m$  using  $^{14}\text{N}$  and  $^{12}\text{C}$  beams of 60–90 MeV and targets of  $fp$ -shell nuclei ( $^{52,53}\text{Cr}$ ,  $^{50}\text{Ti}$ , and  $^{54}\text{Fe}$ ) and of heavy nuclei ( $^{208}\text{Pb}$  and  $^{209}\text{Bi}$ ),<sup>3</sup> the present authors observed that  $Q^m$  does not reflect sharply the structure of individual target nuclei and that, for a given incident beam and target,  $Q^m$  is proportional to the number of transferred nucleons,  $n$ , for  $n \leq 4-5$ .

It is important to identify not only the atomic numbers of the emitted particles,  $b$ , but also of their mass numbers. Very little data has been reported on the systematics of the  $Q^m$  values of individual outgoing nuclides, except for the results of Dubna group for the reactions  $^{232}\text{Th} + ^{15}\text{N}$  [Ref. 1(a)] and  $^{232}\text{Th} + ^{22}\text{Ne}$  [Ref. 1(b)] at fixed energies and at fixed angles and the results previously reported by the present authors.<sup>3</sup> In other studies, including those of  $^{232}\text{Th} + ^{40}\text{Ar}$ ,<sup>2</sup> the  $Q^m$  values of the products either were classified only according to atomic number or were not as extensive.

The present work aims at a more systematic study of the most probable  $Q$  values for a wide range of incident and outgoing variables, i.e., incident beam ( $^{14}\text{N}$  and  $^{12}\text{C}$ ), energy (64–97 MeV),

target mass ( $^{52,53}\text{Cr}$ ,  $^{90}\text{Zr}$ , and all the stable isotopes of molybdenum) and the mass, charge, energy, and angle of emission of emitted particles. The energy and mass region of this study covers the gap of previous data between the sub-Coulomb and high-energy regions. The present authors thus attempt a unified view of the global behavior of multinucleon transfer reactions and the systematics of the most probable  $Q$  values.

Data and detailed discussions on reaction cross sections and angular distributions of reaction products are given in separate papers.<sup>3,12,13</sup>

## II. EXPERIMENTAL PROCEDURE

The present work was performed with  $^{14}\text{N}^{4+}$  beams from the IPCR cyclotron. The experimental facilities and details are described elsewhere.<sup>10-13</sup>

The experimental conditions and measured particles are tabulated in Table I, together with those of previous data.<sup>3</sup> Table I shows the incident channel  $A + a$  of reaction  $A(a, b)B$ , the incident

laboratory and c.m. energies,  $E_{\text{lab}}$  and  $E_i$ , the Coulomb barrier of the incident channel,  $V_C^i$ , and the products  $b$  measured at the laboratory angle  $\theta_{\text{lab}}(b)$ . We chose the radius parameter  $r_0$  to be 1.4 fm.

All targets used in the present work were self-supporting foils, 0.45 to 1 mg/cm<sup>2</sup> thick, of isotopes enriched to more than 90%.

The beam was focused onto the target to a size of  $1 \times 6$  mm<sup>2</sup> and an intensity of 50 to 200 nA.

The reaction products  $b$  were detected with two sets of silicon detector telescopes. The  $\Delta E$  detectors were 30  $\mu\text{m}$  thick and the  $E$  detectors were 200 to 2000  $\mu\text{m}$  thick. All the data were stored on a magnetic tape with the aid of a DDP 124 computer used as in the on-line mode and were later analyzed. The energy spectra of individual  $Z$  and  $A$  were obtained using the program "MTSORT."<sup>13</sup> Thus, using the incident beam of  $^{14}\text{N}$ , isotopes of O, N, C, B, Be, Li, and He were identified by their mass spectra, with a resolution of 3-6%. The overall energy resolution was between 500 and 800 keV.

TABLE I. Multinucleon transfer reactions  $A(a, b)B$  investigated.  $E_{\text{lab}}$  is the incident laboratory energy,  $E_i$  the incident c.m. energy,  $V_C^i$  the Coulomb barrier in the incident channel with the radius parameter  $r_0$  fixed at 1.4 fm, and  $\theta_{\text{lab}}(b)$  the laboratory emission angle of  $b$ .

$A + a$	$E_{\text{lab}}$ (MeV)	$E_i$ (MeV)	$E_i/V_C^i$ ( $r_0=1.4$ fm)	$E_i-V_C^i$ ( $r_0=1.4$ fm)	$b$ measured	$\theta_{\text{lab}}(b)$ (deg)
$^{52}\text{Cr} + ^{14}\text{N}$	95	74.9	2.7	46.7	$^{13}\text{C}, ^{12}\text{C}, ^{12}\text{B}, ^{11}\text{B}, ^{10}\text{B}, ^{10}\text{Be}$	16, 20, 25
	90	70.9	2.5	42.7	$^9\text{Be}, ^7\text{Be}, ^7\text{Li}, ^6\text{Li}, ^4\text{He}$ $^{13}\text{C}, ^{12}\text{C}, ^{12}\text{B}, ^{11}\text{B}, ^{10}\text{B}, ^{10}\text{Be}$	16, 25
	80	63.0	2.2	34.8	$^9\text{Be}, ^7\text{Be}, ^7\text{Li}, ^6\text{Li}, ^4\text{He}$ $^{13}\text{C}, ^{12}\text{C}, ^{12}\text{B}, ^{11}\text{B}, ^{10}\text{B}, ^{10}\text{Be}$	18, 22, 26 18, 22, 27
	70	55.2	2.0	27.0	$^9\text{Be}, ^7\text{Be}, ^7\text{Li}, ^6\text{Li}, ^4\text{He}$ $^{13}\text{C}, ^{12}\text{C}, ^{12}\text{B}, ^{11}\text{B}, ^{10}\text{B}, ^{10}\text{Be}$	22, 27
	64	50.4	1.8	22.2	$^9\text{Be}, ^7\text{Be}, ^7\text{Li}, ^6\text{Li}, ^4\text{He}$ $^{13}\text{C}, ^{12}\text{C}, ^{12}\text{B}, ^{11}\text{B}, ^{10}\text{B}, ^{10}\text{Be}$	20, 27
$^{53}\text{Cr} + ^{14}\text{N}$	90	71.2	2.5	43.2	$^9\text{Be}, ^7\text{Be}, ^7\text{Li}, ^6\text{Li}, ^4\text{He}$ $^{16}\text{O}, ^{15}\text{O}, ^{15}\text{N}, ^{13}\text{C}, ^{12}\text{C},$ $^{11}\text{B}, ^{10}\text{B}, ^{10}\text{Be}, ^9\text{Be},$ $^7\text{Be}, ^7\text{Li}, ^6\text{Li}, ^4\text{He}$	16
$^{50}\text{Ti} + ^{14}\text{N}$	70	54.7	2.1	28.7	$^{13}\text{C}, ^{12}\text{C}, ^{11}\text{B}, ^{10}\text{B}$	25
$^{54}\text{Fe} + ^{14}\text{N}$	70	55.6	1.8	25.3	$^{13}\text{C}, ^{12}\text{C}, ^{11}\text{B}, ^{10}\text{B}$	26
$^{52}\text{Cr} + ^{12}\text{C}$	90	73.1	3.0	48.5	$^{10}\text{B}, ^{10}\text{Be}, ^9\text{Be}, ^7\text{Be}$	18
	70	56.9	2.3	32.3	$^{10}\text{B}, ^{10}\text{Be}, ^9\text{Be}$	18, 22
	60	48.8	2.0	24.2	$^{10}\text{B}, ^{10}\text{Be}, ^9\text{Be}$	17, 19, 22 25, 27
$^{50}\text{Ti} + ^{12}\text{C}$	60	48.4	2.1	25.7	$^{10}\text{B}, ^{10}\text{Be}, ^9\text{Be}$	25
$^{54}\text{Fe} + ^{12}\text{C}$	60	49.1	1.9	22.7	$^{10}\text{B}, ^{10}\text{Be}, ^9\text{Be}$	25
$^{208}\text{Pb} + ^{14}\text{N}$	90	84.3	1.2	13.4	$^{13}\text{C}, ^{12}\text{C}$	60, 65, 70, 75 80, 85
$^{209}\text{Bi} + ^{14}\text{N}$	91	85.3	1.2	13.6	$^{13}\text{C}, ^{12}\text{C}$	60
$^{208}\text{Pb} + ^{12}\text{C}$	78	73.8	1.2	12.2	$^{11}\text{B}, ^{10}\text{Be}, ^9\text{Be}$	75
$^{209}\text{Bi} + ^{12}\text{C}$	78	73.8	1.2	11.5	$^{11}\text{B}, ^{10}\text{Be}, ^9\text{Be}$	70
$^A\text{Mo} + ^{14}\text{N}$	97	84.7	2.0	41.4	$^{16}\text{O}, ^{15}\text{O}, ^{15}\text{N}, ^{13}\text{C}, ^{12}\text{C}, ^{12}\text{B},$ $^{11}\text{B}, ^{10}\text{B}, ^{10}\text{Be}, ^9\text{Be}, ^7\text{Be},$ $^7\text{Li}, ^6\text{Li}, ^4\text{He}$	25, 30
	( $A = 92, 94, 95, 96, 97, 98, 100$ )					
$^{90}\text{Zr} + ^{14}\text{N}$	75	64.9	1.6	23.0	$^{13}\text{C}, ^{12}\text{C}, ^{11}\text{B}$	30, 45
$^{92}\text{Mo} + ^{12}\text{C}$	90	79.6	2.1	41.5	$^{10}\text{B}, ^{10}\text{Be}, ^9\text{Be}, ^7\text{Be}, ^7\text{Li}, ^6\text{Li}$	20

### III. RESULTS AND DISCUSSION

#### A. Experimental results

In Fig. 1, the energy spectra of emitted particles  $b$  from the reaction  $^{96}\text{Mo} + ^{14}\text{N}$  at  $E_{\text{lab}} = 97$  MeV and  $\theta_{\text{lab}} = 25^\circ$  are shown. They are dominated by a continuous bump except for the spectrum of  $^{15}\text{O}$ . The arrows with notations g.s. and  $V_C^f$  indicate the positions of the ground state and the Coulomb barrier in the final channel, respectively. The spectra of the Be and Li isotopes are of a symmetric form, whereas those of the heavier particles are asymmetric and have a tail on the low-energy side. The spectrum of  $^4\text{He}$  is asymmetric but has a tail on the high-energy side.

In order to obtain the angular dependence of  $Q^m$ , the energy spectra of the various emitted particles were measured at the angles listed in Table I.

Figure 2 shows the energy spectra of  $^{12}\text{C}$  from the reaction  $^{53}\text{Cr} + ^{14}\text{N}$  at  $E_{\text{lab}} = 90$  MeV and  $\theta_{\text{lab}} = 15^\circ, 24^\circ,$  and  $27^\circ$ . We see that the bump of the energy spectrum consists of two parts with respect to the energy of emitted particles for  $n \leq 4$ . The higher-energy part has larger cross sections at small angles, while the yield of the lower-energy part is relatively larger at large angles. The following discussion of  $Q^m$  concerns the higher-energy part

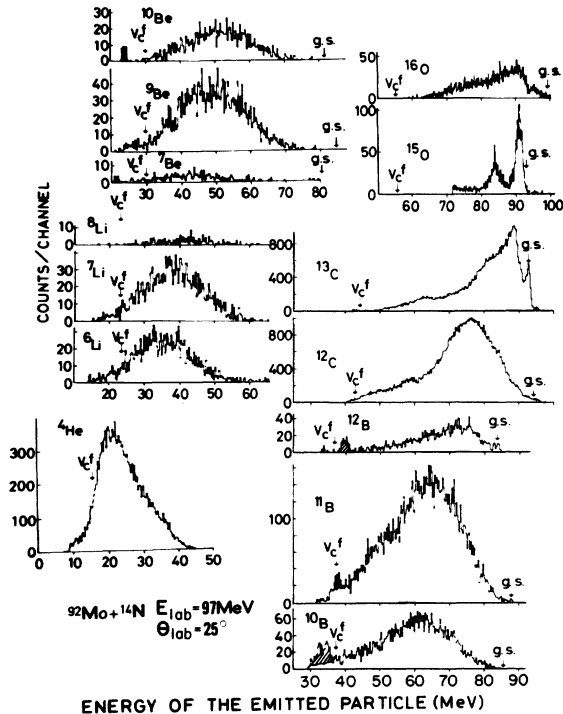


FIG. 1. Energy spectra of emitted particles  $^{16,15}\text{O}$ ,  $^{13,12}\text{C}$ ,  $^{12,11,10}\text{B}$ ,  $^{10,9,7}\text{Be}$ ,  $^{8,7,6}\text{Li}$ , and  $^4\text{He}$  from the reactions  $^{96}\text{Mo} + ^{14}\text{N}$  at  $E_{\text{lab}} = 97$  MeV,  $\theta_{\text{lab}} = 25^\circ$ . The notations g.s. and  $V_C^f$  denote the position of the ground state and the Coulomb barrier in the final channel.

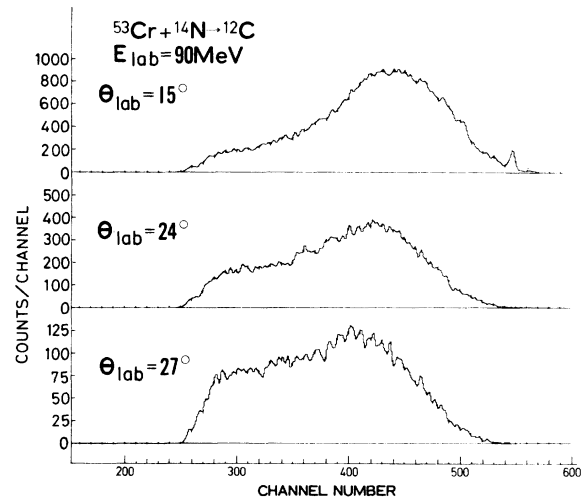


FIG. 2. Energy spectra of  $^{12}\text{C}$  from the reaction  $^{53}\text{Cr} + ^{14}\text{N}$  at  $E_{\text{lab}} = 90$  MeV,  $\theta_{\text{lab}} = 15^\circ, 24^\circ,$  and  $27^\circ$ .

of reactions with  $M_b < M_a$ , when two peaks are present.

Figure 1 also shows that the full width at half maximum (FWHM) of the bump,  $\Gamma$ , for a given set of incident variables increases with  $n$  up to  $\sim 4$  and then decreases for larger  $n$  (see Sec. III B and Tables II and III). This general trend in the spectrum shape and width are partly due to the existence of two components in the energy spectra for  $n \leq 4$ . For a given reaction,  $A(a, b)$ ,  $\Gamma$  increases as the increase of  $E_i$  (see Fig. 3).

The shape of the energy spectrum depends also on the bombarding energy. The variation of the energy spectrum of  $^9\text{Be}$  from the reaction  $^{52}\text{Cr} + ^{12}\text{C}$  at  $E_{\text{lab}} = 60, 70,$  and  $90$  MeV is shown in Fig. 3. It is clearly seen that for an increase in  $E_{\text{lab}}$ , (i) the selective peaks disappear, (ii) the bump shifts toward higher excitation energies, and (iii) the bump broadens.

In order to determine the dependence of the spectrum shape on the target mass, the  $^{14}\text{N}$ -induced reactions were studied for all stable isotopes of molybdenum  $^A\text{Mo}$  ( $A = 92, 94, 95, 96, 97, 98,$  and  $100$ ) at  $E_{\text{lab}} = 97$  MeV and  $\theta_{\text{lab}} = 25^\circ$ . The spectra of the emitted  $^{13}\text{C}$  are shown in Fig. 4. It is seen that gross features of the spectra are very similar.

#### B. Systematics of the most probable $Q$ values $Q^m$

Let us first define some useful  $Q$  values.  $Q^m$  is the  $Q$  value corresponding to the peak position of the bump of the spectrum. The values  $Q_1$  and  $Q_2$  denote the  $Q$  values for which the yields are one-half of the value at  $Q^m$ , corresponding, respectively, to the higher and lower energies of the outgoing particles. Thus,  $\Gamma = Q_1 - Q_2$  gives the

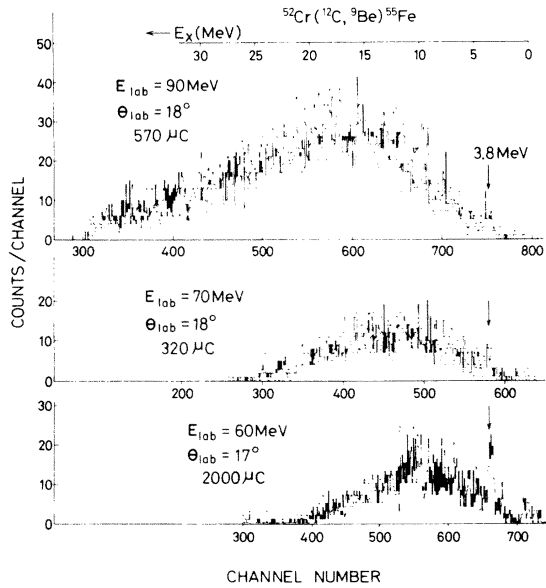


FIG. 3. Energy spectra of  ${}^9\text{Be}$  from  ${}^{52}\text{Cr} + {}^{12}\text{C}$  at  $E_{\text{lab}} = 60, 70,$  and  $90$  MeV.

FWHM of the bump. The  $Q_{gg}$  is the ground state  $Q$  value.

It is often argued<sup>9,14</sup> that in the “stripping-type” transfer reaction, i.e.,  $M_b < M_a$ , the weakly bound lighter product nucleus  $b$  is not excited, so that the high excitation energy  $E_x$  is concentrated in the primary heavy product  $B$ . In such a situation, the relation

$$Q^m = Q_{gg} - E_x^m \quad (1)$$

is obtained, where  $E_x^m$  corresponds to the most probable excitation energy of the heavier product  $B$ . Therefore, the most probable  $Q$  value,  $Q^m$ , the ambiguity of which is estimated to within  $\pm 2$  MeV in most cases, can be obtained.

Table II indicates the  $Q$  values of the reactions  ${}^{52,53}\text{Cr} + {}^{14}\text{N}$ . It shows the  $E_{\text{lab}}$ , identified particle  $b$ , and laboratory angle of emission  $\theta_{\text{lab}}$ . The values of  $Q^m$ ,  $Q_{gg}$ ,  $Q_1$ ,  $Q_2$ , and  $E_x^m$  for each reaction are arranged according to the order of the values of  $\theta_{\text{lab}}$ . When two components in the bump are present,  $Q^m(1)$  and  $Q^m(2)$  denote the  $Q^m$  values corresponding to the higher- and the lower-energy parts, respectively. The  $\bar{Q}_{\text{eff}}^m$  are the “effective”  $Q^m$  values (see Sec. III C) of the higher-energy part averaged over the observed angles. At 90 MeV, the  $\bar{Q}_{\text{eff}}^m$  are averaged over the  ${}^{52}\text{Cr} + {}^{14}\text{N}$  and  ${}^{53}\text{Cr} + {}^{14}\text{N}$  reactions. The table shows that  $E_x^m$  increases with an increase in  $n$ , the number of transferred particles; it is about 10 MeV for  $n = 1$  and about 70 MeV for  $n = 10$ .

Table III compiles the  $Q$  values for the reactions  ${}^A\text{Mo} + {}^{14}\text{N}$  ( $A = 92, 94, 95, 96, 97, 98,$  and  $100$ ),  ${}^{92}\text{Mo}$

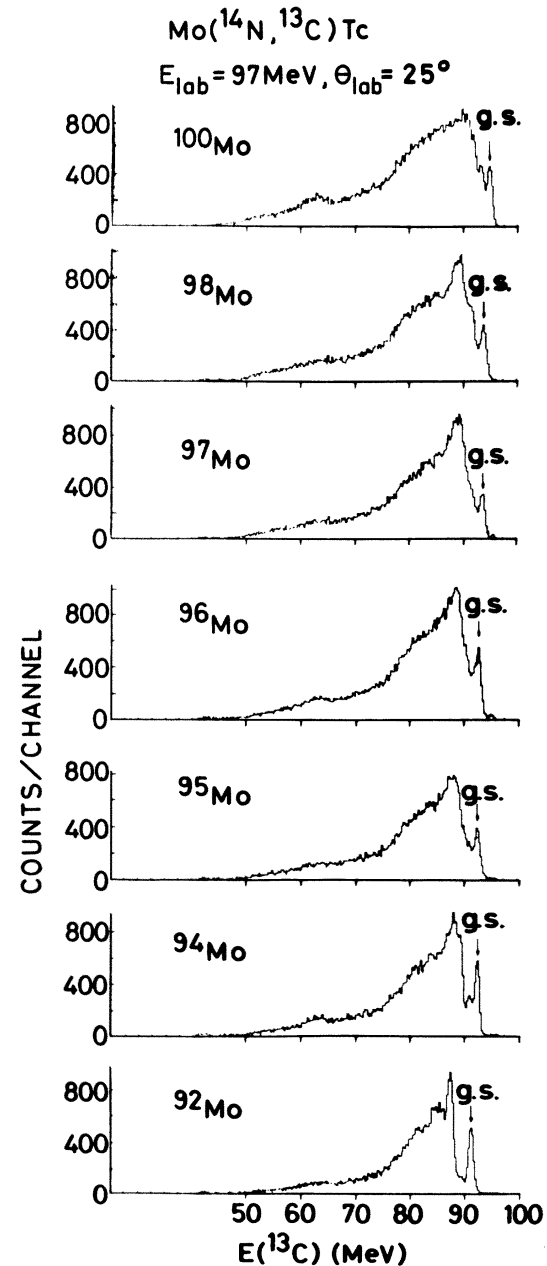


FIG. 4. Energy spectra of  ${}^{13}\text{C}$  from the reactions  ${}^A\text{Mo} + {}^{14}\text{N}$  ( $A = 92, 94, 95, 96, 97, 98,$  and  $100$ ) at  $E_{\text{lab}} = 97$  MeV,  $\theta_{\text{lab}} = 25^\circ$ .

$+ {}^{12}\text{C}$  and  ${}^{90}\text{Zr} + {}^{14}\text{N}$  at  $E_{\text{lab}} = 97, 90,$  and  $90$  MeV, respectively.

#### 1. Dependence of $Q^m$ on $\theta_{\text{lab}}$

As is shown in Tables II and III, the  $Q^m$  for specific reactions do not depend sensitively on the emission angles  $\theta_{\text{lab}}$  of the products. In Fig. 5, the  $Q^m$  of several products in the reaction  ${}^{53}\text{Cr}$

TABLE II.  $Q$  values of the reactions  $^{52,53}\text{Cr} + ^{14}\text{N}$ .  $Q^m$ ,  $Q_1$ ,  $Q_2$ , and  $E_x^m$  are arranged according to the order of the  $\theta_{\text{lab}}$ .  $\bar{Q}_{\text{eff}}^m$  is the value averaged over data for different  $\theta_{\text{lab}}$ . The  $\bar{Q}_{\text{eff}}^m$  preceded by an asterisk and listed as  $^{52}\text{Cr} + ^{14}\text{N}$  denote those values averaged over reactions  $^{52}\text{Cr} + ^{14}\text{N}$  and  $^{53}\text{Cr} + ^{14}\text{N}$ . For the  $^{53}\text{Cr} + ^{14}\text{N}$  reactions,  $Q^m(1)$  and  $Q_{\text{eff}}^m(1)$  correspond to the higher-energy parts, while  $Q^m(2)$  and  $Q_{\text{eff}}^m(2)$  correspond to the lower-energy parts of the continuous spectra.

$A+a$	$E_{\text{lab}}$ (MeV)	$b$	$\theta_{\text{lab}}$ (deg)	$Q_{\text{gg}}$ (MeV)	$Q^m$ (MeV)	$Q_1$ (MeV)	$Q_2$ (MeV)	$\bar{Q}_{\text{eff}}^m$ (MeV)	$E_x^m$ (MeV)			
$^{52}\text{Cr} + ^{14}\text{N}$	95	$^{13}\text{C}$	16, 20, 25	- 1.0	-10.5, -11, -12	-5, -5, -5	-25, -31, -33	- 8.3	9.5, 10, 11			
				+ 3.0	-18, -18.5, -18.5	-9.5, -10, -10	-30, -31, -50	-15.4	21, 21, 21.5			
				- 3.7	-28, -30, -32	-16, -16, -18.5	-43, -41, -46	-23.8	24, 26, 28			
				- 4.0	-36, -36.5, -40	-20, -24, -27	-49, -59, -56	-29.3	32, 32.5, 36			
				- 9.1	- , - , -39	- , - , -29	- , - , -49	-29.2	- , - , -30			
				- 4.3	-42, -44, -43	-28, -33, -29	-54, -47, -57	-33.4	38, 40, 39			
				- 6.1	-47, -49, -51	-36, -38, -40	-56, -59, -61	-39.2	41, 43, 45			
				- 6.3	-48, -48, -48	-37, -38, -39	-60, -60, -59	-34.3	42, 42, 42			
				- 2.2	-52, -54, -55	-43, -46, -44	-63, -65, -68	-39.6	50, 52, 53			
				+ 7.8	- , -64, -66	- , -61, -	- , -69, -	-46.0	- , 72, 74			
			$^{52}\text{Cr} + ^{14}\text{N}$	90	$^{13}\text{C}$	16, 25	- 1.0	-10.5, -10.5	-4, -3	-18, -18.5	*- 7.1	9.5, 10.5
							+ 3.0	-17, -17	-9, -7	-35, -32	-13.9	20, 22
							- 9.7	-20, -19	-12, -	-33, -	-13.1	10, 11
	- 3.7	-27, -30				-15, -24	-40, -47	-21.8	23, 27			
	- 4.0	-32, -29				-20, -21	-48, -47	-23.5	28, 24			
	- 9.1	-33.5, -				-23, -	-48, -	-23.6	23.5, -			
	- 4.3	-37, -				-27, -	-49, -	-27.2	33, -			
	- 6.1	-43.5, -				-27, -	-49, -	-34.0	37.5, -			
	- 6.3	-44				-34, -35	-59, -56	-31.3	38, 43			
	- 2.2	-50, -47				-40, -39	-60, -61	-33.6	48, 45			
	+ 7.8	-58, -57				-52, -52	-65, -62	-40.1	66, 68			
$^{53}\text{Cr} + ^{14}\text{N}$	90	$^{13}\text{C}$				16	+ 0.0	-9	-4.5	-16		9
							+ 5.3	-16.5	-8	-27		22
				- 8.4	-19	-12	-31		9			
				- 0.5	-26	-12	-39		25			
				- 4.3	-28	-20	-41		24			
				- 5.7	-32	-26	-49		26			
				- 3.9	-37	-28	-49		33			
				- 6.5	-44	-	-		37.5			
				- 2.9	-45	-35	-55		42			
				- 2.3	-45	-40	-48		43			
				+10.7	-59	-40	-65		70			
			$^{52}\text{Cr} + ^{14}\text{N}$	80	$^{13}\text{C}$	18, 22, 27	- 1.0	-10, -11.5, -10.5	-5, -6, -4.5	-18, -20, -20	- 7.8	9, 10.5, 9.5
							+ 3.0	-17, -18, -22	-7, -7.5, -8	-30, -29.5, -44	-16.1	20, 21, 25
	- 9.7	-19, -20, -23				-13, -13, -	-25, -27, -	-13.3	9, 10, 19.5			
	- 3.7	-26, -25, -28				-15, -17, -15	-34, -34, -34	-18.5	22, 21.5, 24			
	- 4.0	-31, -31, -32.5				-18, -19, -21	-41, -41, -45	-23.8	27, 27, 28.5			
	- 9.1	- , -30, -				- , -30, -	- , -30, -	-20.2	- , 21, -			
	- 4.3	-32, -34, -32.5				-23, - , -27	-42, - , -42	-23.0	28, 30, 28.5			
	- 6.1	-38, -36, -39				-31, - , -	-46, - , -	-28.0	32, 30, 33			
	- 6.3	-38.5, -39, -39				-30, -32, -31	-48, -51, -48	-25.1	32, 33, 33			
	- 2.2	-43, -43.5, -45				-33, -34, -36	-51, -53, -54	-30.3	41, 41.5, 43			
	+ 7.8	-52, -51, -53				-49, -48, -47	-57, -56, -59	-34.3	60, 59, 60.5			
$^{52}\text{Cr} + ^{14}\text{N}$	70	$^{13}\text{C}$				22, 27	- 1.0	-10, -8.5	-4.5, -4	-14.5, -15	- 6.4	9, 7.5
							+ 3.0	-14, -13	-6, -5	-25, -26	-10.6	17, 16
				- 9.7	-16, -	-11, -	-21, -	- 9.8	6.5, -			
				- 3.7	-19, -19	-12, -11	-25.5, -26	-12.8	15, 15.5			
				- 4.0	-27, -28.5	-17, -18	-34, 37	-21.6	23, 24.5			
				- 4.3	-28, -28	-21, -22	-36, -33	-18.2	24, 24			
				- 6.1	-32, -33	-21, -	-36, -	-22.7	25, 27			
				- 6.3	-32, -34	-24, -	-41, -	-19.3	26, 28			
				- 2.2	-36, -35	-29, -28	-45, -45	-21.8	34, 33			
				+ 7.8	-44, -44	-41, -38	-48, -48	-26.1	51.5, 51.5			

TABLE II. (Continued)

$A+a$	$E$ (MeV)	$b$	$\theta_{\text{lab}}$ (deg)	$Q_{\text{eff}}$ (MeV)	$Q^m$ (MeV)	$Q_1$ (MeV)	$Q_2$ (MeV)	$\bar{Q}_{\text{eff}}^m$ (MeV)	$E_x^m$ (MeV)
$^{52}\text{Cr} + ^{14}\text{N}$	64	$^{13}\text{C}$	20, 27	- 1.0	-8, -7	-2, -2	-13, -12	- 4.6	7, 6
				+ 3.0	-12.5, -14	-4, -4	-20.5, -21	-10.4	15.5, 17
				- 9.7	-14, -			- 7.6	4, -
				- 3.7	-16, -17	-9, -9	-23, -23.5	-10.3	12, 13
				- 4.0	-22, -23	-15, -14	-29, 5, -30	-16.3	18, 19
				- 4.3	-24, -25	-18, -	-30, -	-14.5	20, 21
				- 6.1	-27, -29			-18.0	21, 23
				- 6.3	-30, -31	-24, -25	-35, -36	-16.8	24, 25
				- 2.2	-32, -33.5	-23, -23	-41, -41	-19.1	30, 31.5
				+ 7.8	-38, -39	-35, -33	-43, -44	-20.6	46, 46.5
$^{53}\text{Cr} + ^{14}\text{N}$	90	$^{13}\text{C}$	15	+0.0	- 8.5	- 5.5	-23	-20	
			18		-10	- 7	-24	-21	
			21		-11	- 8	-26	-23	
			24		-11.5	- 8.5	-26.5	-23.5	
			27		-12	- 9	-28	-25	
			30		-14	-11	-30.5	-27.5	
			$^{12}\text{C}$	10	+5.3	-16.5	-13.5		
				12		-16	-13	-33	-30
				15		-17	-14	-34	-31
				18		-17	-14	-36	-33
21		-18		-15	-35	-32			
24		-18		-15	-35	-32			
27		-18		-15	-34	-31			
$^{11}\text{B}$	30		-19	-16	-34	-31			
	33		-18.5	-15.5	-34	-31			
	10	-0.5	-26	-20	-38.5	-32			
	12		-25	-19	-37	-31			
	15		-26.5	-20					
	18		-26.5	-20	-40	-34			
	21		-28.5	-22	-40	-34			
	24		-30	-24	-42	-36			
	27		-30.5	-24					
	30		-32.5	-26					
$^{10}\text{B}$	33		-33.5	-27					
	10	-4.3	-29	-23	-42	-36			
	12		-29	-23	-40	-34			
	15		-29	-23	-41	-35			
	18		-30	-24					
	21		-32	-26					
	24		-33	-27					
	27		-33	-27					
	30		-34	-28	-41.5	-35			
	33		-36	-30					
$^9\text{Be}$	12	-3.9	-37.5	-28					
	15		-38	-28					
	18		-38	-28					
	21		-39	-28					
	24		-38.5	-29					
	27		-39	-29					
	30		-39.5	-30					
	33		-40	-30					

TABLE III.  $Q$  values of the reactions  ${}^A\text{Mo}+{}^{14}\text{N}$ ,  ${}^{92}\text{Mo}+{}^{12}\text{C}$ ,  ${}^{80}\text{Zr}+{}^{14}\text{N}$ .  $Q^m$ ,  $Q_1$ ,  $Q_2$ , and  $Q_{\text{eff}}^m$  are arranged according to the order of the  $\theta_{\text{lab}}$ .

${}^A\text{Mo}+{}^{14}\text{N}, E_{\text{lab}} = 97 \text{ MeV}, \theta_{\text{lab}} = 25^\circ, 30^\circ$						
$A$	$b$	$Q_{\text{eff}}$ (MeV)	$Q^m$ (MeV)	$Q_1$ (MeV)	$Q_2$ (MeV)	$Q_{\text{eff}}^m$ (MeV)
92	${}^{13}\text{C}$	- 3.5	- 7.5, - 9.7	- 7, - 7	-14, -16	- 2.4, - 4.6
94		- 2.7	- 6.5, - 8.4	- 6, - 6	-15, -18	- 1.4, - 3.3
95		- 2.1	- 6.6, - 8.5	- 5, - 6	-16, -18	- 1.5, - 3.4
96		- 1.9	- 6.3, - 8.0	- 4, - 4	-16, -18	- 1.2, - 2.9
97		- 1.3	- 6.1, - 8.4	- 3, - 4	-14, -19	- 1.0, - 3.3
98		- 1.0	- 5.5, - 8.4	- 3, - 3	-16, -20	- 0.4, - 3.3
100		- 0.1	- 6.3, - 8.9	- 1, - 3	-18, -19	- 1.2, - 3.7
Mean			- 7.5	- 4	-17	- 2.5
92	${}^{12}\text{C}$	+ 0.2	-18.4, -18.1	-10, -10	-26, -27	-13.3, -13.0
94		+ 0.3	-18.4, -17.8	-10, -10	-28, -27	-13.3, -12.7
95		+ 2.4	-18.3, -18.1	-10, -10	-27, -28	-13.2, -13.0
96		+ 0.6	-18.2, -17.6	-10, - 9	-27, -27	-13.1, -12.5
97		+ 2.7	-18.3, -18.1	-10, -10	-27, -28	-13.2, -13.0
98		+ 0.6	-18.1, -17.5	-10, - 9	-27, -27	-13.0, -12.4
100		+ 1.3	-18.1, -17.5	- 9, - 9	-27, -27	-13.0, -12.4
Mean			-18.1	-9.5	-27	-13.0
92	${}^{12}\text{B}$	-14.8	-22.2, -24.1	-18, -19	-34, -35	-13.5, -11.6
94		-12.8	-23.0, -24.3	-16, -17	-35, -34	-13.7, -12.4
95		-12.2	-21.6, -23.2	-16, -18	-35, -32	-12.6, -11.0
96		-11.1	-21.4, -23.5	-16, -17	-35, -35	-12.9, -10.8
97		-10.4	-21.2, -22.9	-15, -17	-36, -36	-12.3, -10.6
98		- 9.4	-20.6, -23.0	-14, -15	-37, -35	-12.4, -10.0
100		- 7.6	-20.4, -23.1	-13, -15	-38, -37	-12.5, - 9.8
Mean			-22.7	-16	-35	-12.1
92	${}^{11}\text{B}$	- 9.2	-28.4, -29.6	-18, -20	-42, -42	-17.8, -19.0
94		- 8.2	-29.2, -28.5	-19, -21	-43, -41	-18.6, -17.9
95		- 5.3	-29.3, -28.9	-19, -20	-43, -43	-18.7, -18.3
96		- 7.0	-29.4, -28.8	-19, -20	-43, -43	-18.8, -18.2
97		- 4.1	-28.6, -28.9	-19, -20	-43, -44	-18.2, -18.3
98		- 6.0	-29.1, -28.0	-18, -19	-45, -45	-18.5, -17.2
100		- 4.7	-27.8, -27.9	-18, -19	-45, -44	-17.2, -17.3
Mean			-28.8	-19	-43	-18.2
92	${}^{10}\text{B}$	- 9.9	-31.6, -31.8	-22, -22	-44, -46	-21.0, -21.2
94		- 9.4	-31.7, -32.5	-22, -25	-48, -42	-21.1, -21.9
95		- 9.3	-31.3, -30.8	-22, -22	-45, -47	-20.7, -20.2
96		- 8.8	-31.8, -31.0	-22, -22	-45, -45	-21.2, -20.4
97		- 8.8	-31.1, -31.6	-22, -23	-45, -46	-20.5, -21.0
98		- 8.2	-32.0, -32.0	-22, -23	-49, -50	-21.4, -21.4
100		- 7.3	-32.0, -31.8	-21, -22	-48, -47	-21.4, -21.2
Mean			-31.6	-22	-46	-21.0
92	${}^{10}\text{Be}$	-16.9	-38.8, -42.6	-33, -34	-48, -51	-22.5, -26.3
94		-15.0	-41.7, -42.2	-32, -32	-53, -52	-25.4, -25.9
95		-11.9	-41.2, -42.0	-31, -33	-52, -53	-24.9, -25.7
96		- 8.8	-41.3, -42.2	-32, -33	-53, -53	-25.0, -25.9
97		- 8.8	-41.8, -43.7	-30, -33	-55, -54	-25.5, -27.4
98		-11.1	-41.9, -43.3	-30, -32	-53, -54	-25.6, -27.0
100		- 9.0	-41.5, -42.8	-30, -32	-54, -55	-25.2, -26.5
Mean			-42.0	-32	-53	-25.6

TABLE III. (Continued)

$A$	$b$	$Q_{gg}$ (MeV)	$Q^m$ (MeV)	$Q_1$ (MeV)	$Q_2$ (MeV)	$Q_{\text{eff}}^m$ (MeV)
92	${}^9\text{Be}$	-12.7	-43.2, -44.6	-32, -35	-54, -56	-26.9, -28.3
94		-11.3	-43.9, -45.1	-32, -34	-55, -56	-27.6, -28.8
95		-10.6	-43.6, -44.8	-33, -34	-55, -57	-27.3, -28.5
96		- 9.9	-43.7, -44.1	-33, -34	-56, -56	-27.4, -27.8
97		- 9.3	-44.8, -45.1	-33, -34	-56, -56	-28.5, -28.8
98		- 8.6	-44.6, -45.5	-34, -35	-56, -57	-28.3, -29.2
100		- 6.8	-45.2, -45.5	-34, -34	-56, -57	-28.9, -29.2
Mean			-44.5	-33	-56	-28.3
92	${}^7\text{Be}$	-14.2	-50.0, -50.7	-42, -42	-59, -60	-33.7, -34.4
94		-13.9	-50.1, -51.0	-43, -43	-59, -61	-33.8, -34.7
95		-13.8	-49.0, -51.0	-40, -42	-60, -61	-32.7, -34.7
96		-13.7	-48.0, -50.9	-41, -41	-59, -61	-31.7, -33.8
97		-13.5	-51.2, -51.1	-42, -43	-59, -62	-34.9, -34.8
98		-13.2	-52.3, -52.5	-45, -42	-64, -	-36.0, -36.2
100		-12.2	-51.6, -50.4	-43, -42	-63, -	-35.3, -34.1
Mean			-50.7	-42	-61	-34.4
92	${}^7\text{Li}$	-16.7	-53.5, -55.6	-44, -45	-62, -65	-30.1, -33.2
94		-15.0	-53.9, -55.7	-45, -45	-64, -66	-31.5, -33.3
95		-11.8	-54.0, -55.0	-44, -45	-64, -65	-31.6, -33.1
96		-13.4	-54.0, -55.6	-44, -45	-64, -64	-31.6, -33.2
97		-10.2	-54.1, -55.7	-44, -46	-64, -65	-31.3, -33.3
98		-11.7	-54.5, -55.3	-44, -45	-64, -65	-32.1, -32.9
100		- 9.9	-54.6, -55.7	-45, -45	-64, -65	-32.2, -33.3
Mean			-54.8	-45	-64	-32.3
92	${}^6\text{Li}$	-12.8	-57.0, -57.8	-48, -48	-67, -68	-34.7, -35.5
94		-11.7	-58.3, -58.3	-48, -48	-68, -70	-36.0, -36.0
95		-11.5	-56.7, -57.6	-47, -48	-67, -67	-34.4, -35.3
96		-13.4	-56.1, -56.6	-47, -47	-66, -66	-33.8, -34.3
97		-10.4	-56.5, -58.1	-48, -49	-67, -68	-34.1, -35.8
98		- 9.4	-57.5, -59.3	-48, -49	-69, -72	-35.2, -37.0
100		- 7.9	-57.7, -59.5	-48, -49	-69, -71	-35.4, -37.2
Mean			-57.6	-48	-68	-35.3
92	${}^4\text{He}$	- 4.0	-68.2, -69.1	-60, -62	-73, -73	-39.5, -40.4
94		- 2.7	-68.6, -69.3	-59, -62	-74, -74	-39.9, -40.6
95		- 0.2	-68.4, -69.0	-60, -62	-73, -73	-39.7, -40.3
96		- 1.4	-68.4, -68.9	-60, -62	-73, -74	-39.7, -40.2
97		+ 1.3	-68.3, -69.0	-60, -61	-73, -73	-39.6, -40.3
98		- 0.1	-68.6, -69.1	-60, -62	-74, -74	-39.9, -40.4
100		+ 1.7	-68.4, -68.2	-59, -60	-74, -74	-39.7, -40.1
Mean			-68.7	-60.5	-73	-46.0
${}^{92}\text{Mo} + {}^{12}\text{C}, E_{\text{lab}} = 90 \text{ MeV}, \theta_{\text{lab}} = 20^\circ$						
	${}^{10}\text{B}$	-14.7	-22	-17	-32	-16
	${}^{10}\text{Be}$	-16.9	-25	-20	-34	-13
	${}^9\text{Be}$	-14.7	-29	-22	-38	-17
	${}^7\text{Be}$	-16.5	-44	-34	-53	-32
	${}^7\text{Li}$	-19.2	-46	-36	-56	-29
	${}^6\text{Li}$	-17.7	-51	-42	-60	-34
${}^{90}\text{Zr} + {}^{14}\text{N}, E_{\text{lab}} = 75 \text{ MeV}, \theta_{\text{lab}} = 30.5^\circ$						
	${}^{13}\text{C}$	- 2.4	- 8.0	- 5.5	-12.8	- 3.3
	${}^{12}\text{C}$	+ 0.6	-12.4	- 7.2	-20.4	- 7.3
	${}^{11}\text{B}$	- 7.8	-20.5	-13.8	-28.4	-10.3

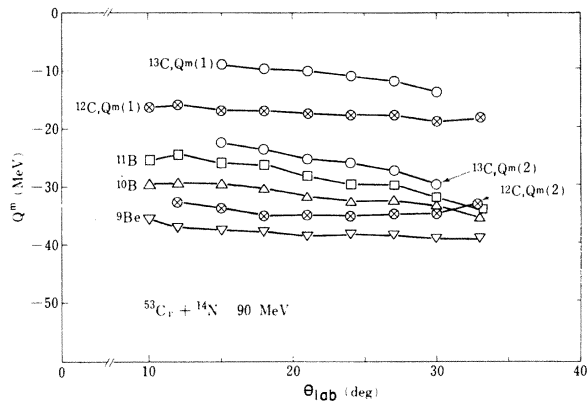


FIG. 5. The most probable  $Q$  values  $Q^m$  of the reactions  $^{53}\text{Cr} + ^{14}\text{N}$  at  $E_{\text{lab}} = 90$  MeV as function of the angle of emission  $\theta_{\text{lab}}$ . For  $^{13}\text{C}$  and  $^{12}\text{C}$ , the  $Q^m$  values of higher- and lower-energy components are shown.

$+ ^{14}\text{N}$  at 90 MeV are plotted against  $\theta_{\text{lab}}$ . This shows more clearly the weak dependence of  $Q^m$  on  $\theta_{\text{lab}}$  over a wide range of  $\theta_{\text{lab}}$ .

For  $^A\text{Mo} + ^{14}\text{N}$  reactions, the largest differences in the  $Q^m$  at  $25^\circ$  and  $30^\circ$  are for  $^{13}\text{C}$  and  $^{12}\text{B}$  and about 2 MeV, which is still small compared with the width,  $\Gamma$ , of the bump. For other  $b$ , the  $Q^m$  are almost the same at the two angles. This can be clearly seen in Fig. 6 in which the four  $Q$  values  $Q^m$ ,  $Q_1$ ,  $Q_2$ , and  $Q_{gg}$  of the reactions  $^A\text{Mo} + ^{14}\text{N}$  at  $\theta_{\text{lab}} = 25^\circ$  and  $30^\circ$  are shown. This situation is in contrast with the case for sub-Coulomb or near-Coulomb reactions, where the “optimum”  $Q$  values are strongly dependent on the emission angles.<sup>5</sup> The  $Q^m$  values of the present study coincide with none of the optimum  $Q$  values cited above<sup>4,5,6</sup> (see Ref. 12). In the study of the reactions  $\text{Ag} + ^{14}\text{N}$  at  $E_{\text{lab}} = 100, 160,$  and  $250$  MeV, Moretto *et al.*,<sup>15</sup> found  $Q^m$  to be independent of  $\theta_{\text{lab}}$ . In research on the  $^{58}\text{Ni}(^{16}\text{O}, ^{12}\text{C})$  reaction above the Coulomb barrier ( $E_{\text{lab}} = 60, 72,$  and  $81$  MeV), Wilczyński *et al.*<sup>16</sup> found that  $Q^m$  changes with angle  $\theta_{\text{c.m.}}$  when  $\theta_{\text{c.m.}}$  is larger than  $\theta_{\text{gr}}$ , grazing angle, while  $Q^m$  remains unchanged at smaller angles, which is consistent with the results of the present study.

## 2. Dependence of $Q^m$ on adjacent $A$

Another aim of this study is to determine the dependence of  $Q^m$  on  $A$ . It was confirmed that the difference of the  $Q^m$  for specific reactions ( $a, b$ ) at the same  $E_i$  is very small compared with that of the  $Q_{gg}$  for  $A = ^{52}\text{Cr}, ^{53}\text{Cr}, ^{50}\text{Ti},$  and  $^{54}\text{Fe}$  (Ref. 3(a) and Table II). For all the stable isotopes of molybdenum, the  $Q^m$  are almost constant for all individual  $A(a, b)$ , as is shown in Fig. 6 and Table

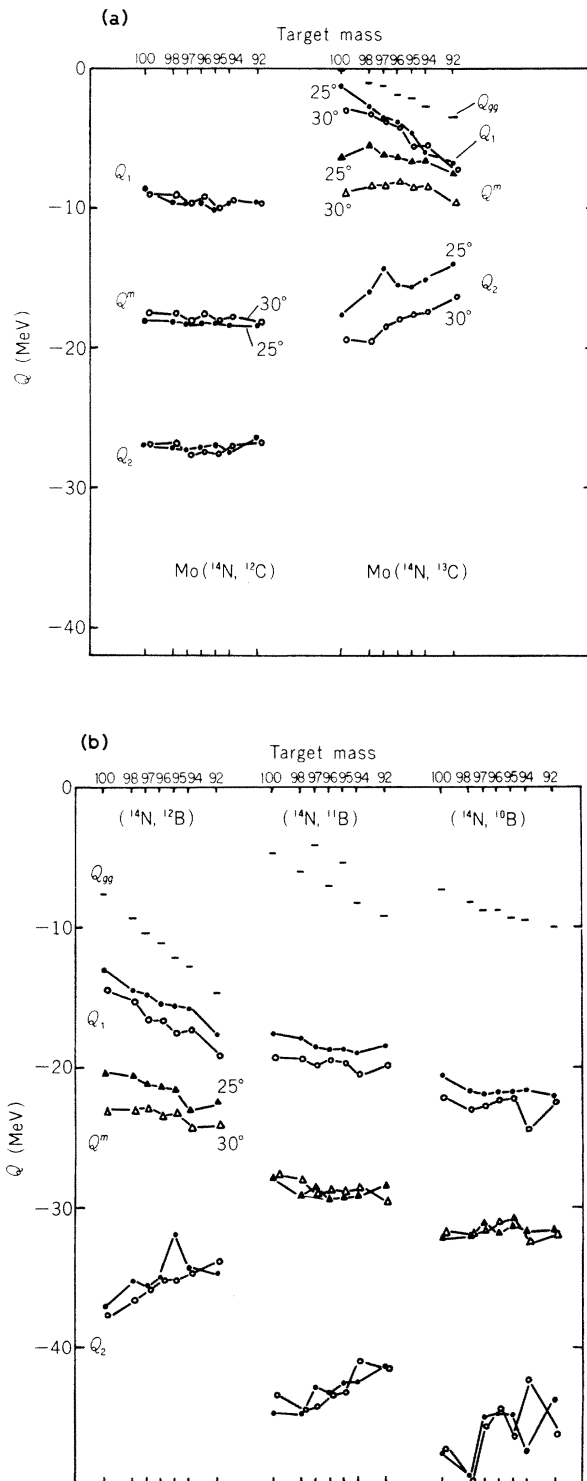


FIG. 6. The most probable and half-maximum  $Q$  values  $Q^m$ ,  $Q_1$ , and  $Q_2$  in the reaction (a)  $(^{14}\text{N}, ^{13}\text{C})$ ,  $(^{14}\text{N}, ^{12}\text{C})$ ; (b)  $(^{14}\text{N}, ^{12}\text{B})$ ,  $(^{14}\text{N}, ^{11}\text{B})$ , and  $(^{14}\text{N}, ^{10}\text{B})$  on Mo isotopes vs mass number of target. The ground state  $Q_{gg}$  values are also shown.

III, despite the large differences in  $Q_{\text{eff}}$ . That  $Q^m$  is independent of adjacent  $A$  has been reported for the reactions  $^A\text{Ni}(^{18}\text{O}, ^{16}\text{O})$  ( $A = 58, 60, 62, \text{ and } 64$ ) at  $E_{\text{lab}} = 63$  MeV and  $\theta_{\text{lab}} = 30^\circ$ .<sup>17</sup>

### 3. Dependence of $Q^m$ on $E_i$ and $n$

Figure 7 shows the variation of  $Q^m$  in the reaction  $^{52}\text{Cr} + ^{14}\text{N}$  with incident laboratory energy  $E_{\text{lab}}$ . For small  $n$ ,  $Q^m$  is almost constant throughout the entire energy range, while with an increase in  $n$ , the absolute value  $Q^m$  and the gradient of  $|Q^m|$  vs  $E_{\text{lab}}$  increase.

Figure 8 is a plot of  $Q^m$  vs  $n$  for the reactions  $^{52,53}\text{Cr} + ^{14}\text{N}$ . A linear relation,

$$Q^m = \alpha n + \beta, \quad (2)$$

is obtained up to a given number of transferred nucleons:  $n \leq 4-5$ . The values of  $\alpha$  and  $\beta$  are given in the inset in the upper-right-hand corner of Fig. 8. For the reactions studied here  $\alpha$  is linear in the incident energy  $E_i$  and lies between  $-5$  and  $-8$  MeV/nucleon, whereas  $\beta$  is independent of  $E_i$  and has a value of about  $-3$  MeV. Note that these relations hold irrespective of proton or neutron transfer, although the  $Q_{\text{eff}}$  are quite different for isobaric product pairs, such as  $^{12}\text{C}$  and  $^{12}\text{B}$ ,  $^{10}\text{B}$  and  $^{10}\text{Be}$ , and  $^7\text{Be}$  and  $^7\text{Li}$ .

This variation of  $Q^m$  with  $E_i$  is not compatible with the prediction of Wilczyński<sup>9</sup> based on the determination of  $Q^m$  from known quantities, i.e., the separation energies of the transferred nucleons from the projectile in "stripping-type" reactions.

A plot similar to that in Fig. 8 for the reactions  $^{92,100}\text{Mo} + ^{14}\text{N}$  at  $E_{\text{lab}} = 97$  MeV [see, e.g., Fig. 2 of Ref. 3(c)] shows a splitting for isobars and a grouping according to the atomic number of  $b$ . This suggests the increasing importance of Cou-

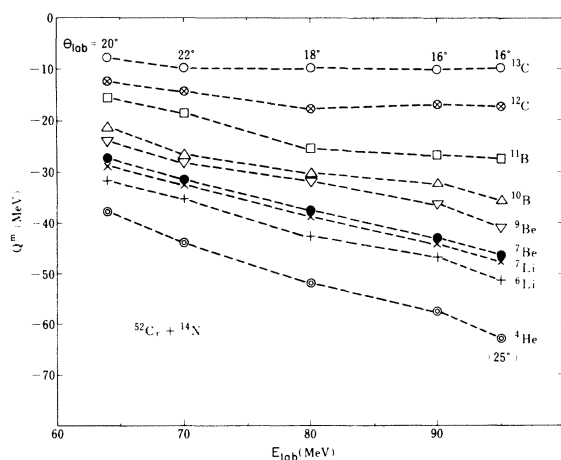


FIG. 7. The most probable  $Q$  values  $Q^m$  of the reactions  $^{52}\text{Cr} + ^{14}\text{N}$  as a function of the bombarding energy  $E_{\text{lab}}$ .

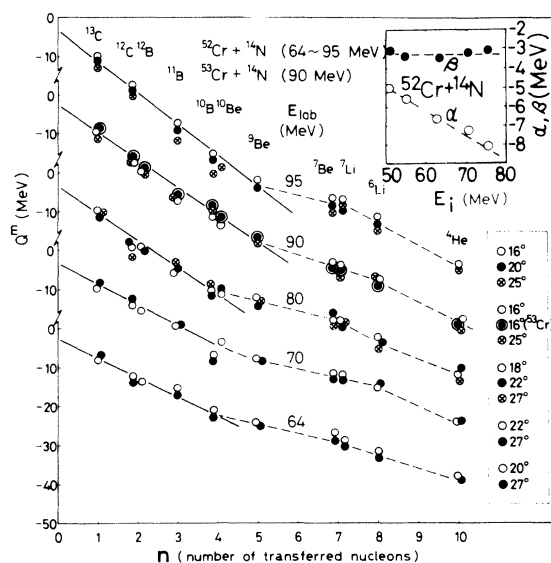


FIG. 8. The most probable  $Q$  values  $Q^m$  of the reactions  $^{52,53}\text{Cr} + ^{14}\text{N}$  as function of the number of transferred nucleons  $n$ . In the upper right part the values of  $\alpha$  of Eq. (2) are plotted vs incident c.m. energy  $E_i$ .

lomb effects which leads us to the following discussion of the effective  $Q$  values.

### C. Systematics of most probable effective $Q$ values $Q_{\text{eff}}^m$

In heavy-ion reactions, because of large difference between the Coulomb barriers of the incident and exit channels, Buttke and Goldfarb<sup>4</sup> and Brink<sup>7</sup> have introduced the concept of "effective  $Q$  values"  $Q_{\text{eff}}$ . It is defined as the  $Q$  value corrected for the difference  $\Delta V = V_C^i - V_C^f$  in the Coulomb barriers between incident and outgoing channels.

#### 1. Dependence of $Q_{\text{eff}}^m$ on $n$ and $E_i$

Figure 9 is a plot of the most probable effective  $Q$  values,  $Q_{\text{eff}}^m$  vs  $n$  for the reactions  $^{52}\text{Cr} + ^{14}\text{N}$  and  $^A\text{Mo} + ^{14}\text{N}$ ,  $A = 92-100$ . The  $Q_{\text{eff}}^m$  are averaged over the angles  $\theta_{\text{lab}}$  and the target isotopes and are compiled in Tables II and III. Figure 9 also shows similar plots for the data of the Dubana group<sup>1,9</sup> for the reactions  $^{232}\text{Th} + ^{15}\text{N}$  at  $E_{\text{lab}} = 145$  MeV and  $^{232}\text{Th} + ^{22}\text{Ne}$  at  $E_{\text{lab}} = 174$  MeV. The data for  $^{232}\text{Th}(^{15}\text{N}, ^{14}\text{N})$  at  $E_{\text{lab}} = 98.5$  MeV<sup>18</sup> is also shown for reference. Except for some discrepancies between  $^{12}\text{C}$  and  $^{12}\text{Be}$ , and  $^{11}\text{B}$  and  $^{11}\text{Li}$  in the reaction  $^{232}\text{Th} + ^{15}\text{N}$ , all the data follow the linear relation

$$Q_{\text{eff}}^m = \alpha_{\text{eff}} n + \beta_{\text{eff}} \quad (3)$$

for  $n \leq 4-5$ . The radius parameter  $r_0$  was chosen to be 1.4 fm. (For reactions with lower  $V_C^i$  and

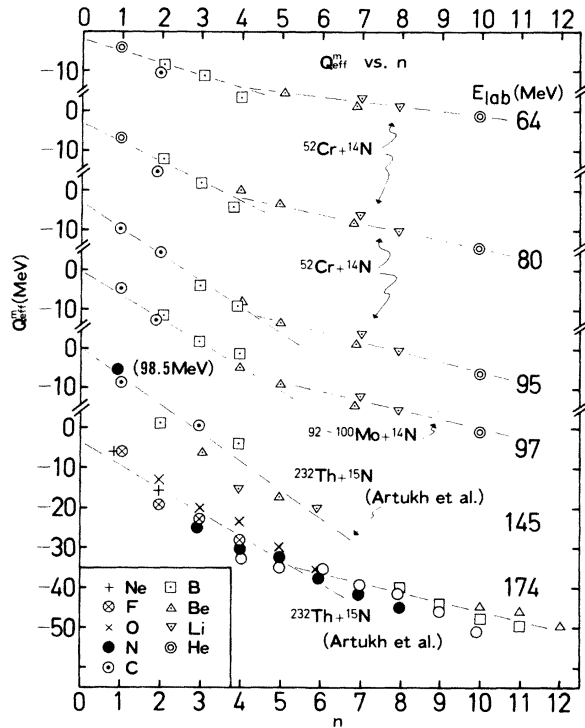


FIG. 9. The most probable effective  $Q$  values  $Q_{\text{eff}}^m$  of the reactions  $^{52}\text{Cr} + ^{14}\text{N}$  and  $^{92-100}\text{Mo} + ^{14}\text{N}$  as function of transferred nucleons  $n$ . The data are averaged over angles and target isotopes. The  $Q_{\text{eff}}^m$  values of the reactions  $^{232}\text{Th} + ^{15}\text{N}$  and  $^{232}\text{Th} + ^{22}\text{Ne}$  of Dubna data are also plotted vs  $n$ .

$E_{\text{lab}}$ , i.e.,  $^{52}\text{Cr} + ^{14}\text{N}$  at  $E_{\text{lab}} = 64$  and  $70$  MeV, the linear relation (2) holds rather better than that of relation (3). In these cases,  $r_0$  should be large, e.g.,  $r_0 \approx 2$  fm. On the other hand, for reactions with high  $V_C^i$ , i.e.,  $^{232}\text{Th} + ^{22}\text{Ne}$ ,  $r_0$  should be small, e.g.,  $r_0 \approx 1.2$  fm. As a compromise,  $r_0 = 1.4$  fm was employed throughout.) The gradient of linear relation (3),  $\alpha_{\text{eff}}$ , is plotted against  $E_i - V_C^i$  in Fig. 10. This figure also includes the data for  $^{90}\text{Zr} + ^{14}\text{N}$  at  $E_{\text{lab}} = 75$  MeV. This plot gives a linear relation

$$\alpha_{\text{eff}} = -0.1(E_i - V_C^i) - 0.9(\text{MeV}). \quad (4)$$

The data for the segment  $\beta_{\text{eff}}$  of the linear relations (3) are scattered between 0 and  $-5$  MeV but are around  $-3$  MeV for  $^{52,53}\text{Cr} + ^{14}\text{N}$  reactions.

It is possible to rewrite  $Q_{\text{eff}}^m$  as

$$\begin{aligned} Q_{\text{eff}}^m &= (E_f^m - V_C^f) - (E_i - V_C^i) \\ &= Q_{\text{eff}}^m + \Delta V_C = Q_{\text{eff}}^m - E_x^m + \Delta V_C = E_f^m - E_i + \Delta V_C \\ &= \Delta E^m + \Delta V_C, \end{aligned} \quad (5)$$

where  $E_f^m$  and  $\Delta E^m$  are the most probable kinetic energies in the exit channel and the most probable

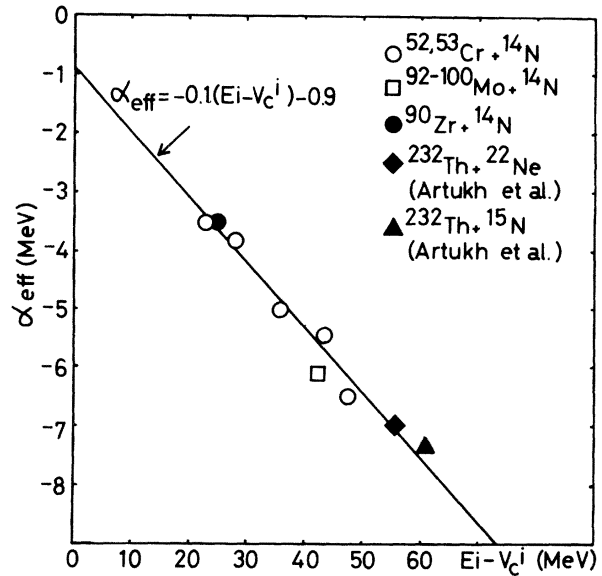


FIG. 10. The  $\alpha_{\text{eff}}$  values of Eq. (2) plotted vs effective incident energy  $E_i - V_C^i$ .

energy loss of the scattering particle, respectively. Relation (3) reflects the fact that, as long as  $n$  is not too large, i.e.,  $n \leq 4-5$ , a constant amount of kinetic energy per nucleon is transferred during the "stripping" and this constant rate,  $\alpha_{\text{eff}}$ , is proportional to the energy available at the barrier,  $E_i - V_C^i$ . This situation holds throughout a wide range of incident variables when  $E_i$  is large compared with  $V_C^i$ . The segment  $\beta_{\text{eff}}$  may correspond to the energy loss of the projectile in the nuclear matter due to inelastic processes,<sup>3</sup> although it is still difficult to form a systematic view on this point.

The simple dependence for  $Q_{\text{eff}}^m$  with respect to  $E_i$ ,  $A$ ,  $n$ , and  $\theta_{\text{lab}}$  were obtained without introduction of the difference in the nuclear potentials at the initial and the final channels as proposed by Siemens *et al.*<sup>3</sup> The systematics of  $Q^m$  are qualitatively understood with the recent interpretation of Wilczyński *et al.*<sup>16</sup> in terms of nuclear friction, with the radial component being much more important than the tangential component.

As is shown in Fig. 1, the cross sections for the production of  $b$  for a given incident channel and energy are very different from one product to another. The most important factor which governs the reaction mechanism, and hence the  $Q^m$ , is the energy loss of the scattering particle in the nuclear matter. The key factors which determine the cross section  $\sigma$  are the  $\Gamma$ , the  $Q_{\text{eff}}$  and the level density of the residual nucleus around excitation  $E_x^m$ ; the spectral form is qualitatively reproduced.<sup>3,13,14</sup>

### 2. Most probable effective outgoing velocity $v_f^m$

In the transfer region, the initial velocity  $v_i$  and the most probable outgoing velocity  $v_f^m$ , at the barrier corresponding to  $Q_{\text{eff}}^m$ , are obtained from the relations

$$\begin{aligned} \frac{1}{2}\mu_i v_i^2 &= E_i - V_C^i, \\ \frac{1}{2}\mu_f (v_f^m)^2 &= E_f^m - V_C^f \\ &= E_i - V_C^i + Q_{\text{eff}}^m \\ &= \frac{1}{2}\mu_i v_i^2 + Q_{\text{eff}}^m, \end{aligned} \quad (6)$$

where  $\mu_i$  and  $\mu_f$  are the reduced masses in each channel.

Figure 11 shows the ratios  $v_f^m/v_i$  plotted against  $n$  for various reactions. The values of  $v_f^m$  are averaged over the emission angles. The general trend is very similar for a wide range of reactions listed in the figure: The ratio  $v_f^m/v_i$  decreases from about unity for  $n=1$  to 0.4–0.5 for  $n=10$ . This is in contrast with the simple theories (e.g., Ref. 7) which assume that the reaction be direct and that  $v_f \approx v_i$ .

The possibility of contributions from the sequential particle decay of excited primary fragments, as proposed by Bondorf and Nörenberg,<sup>19</sup> would result in a constant average velocity  $v_f^m$ , which is not the case in the present experiment.

Since the pioneer work of the Orsay<sup>20</sup> and Dubna groups,<sup>2</sup> it is well known that the spectrum of  $b$  consists of two parts which are called "quasi-elastic" and "deep inelastic" processes. The present authors have also observed the existence of two parts in the spectrum as mentioned above. The higher energy part of this spectrum corresponds to a "quasielastic" process; however, Fig. 11 throws some doubt on the term "quasi-elastic" at least for larger  $n$ .

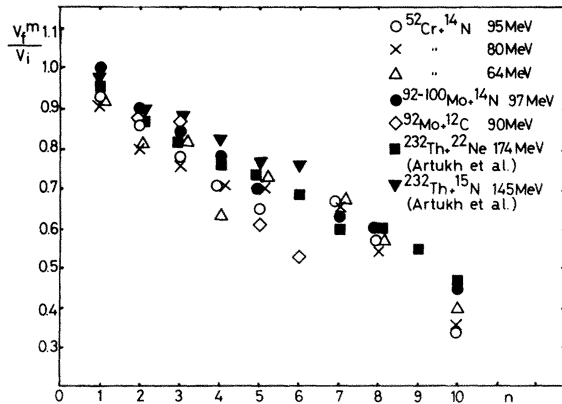


FIG. 11. The ratio of the most probable final velocity  $v_f^m$  to the incident velocity  $v_i$  in the transfer region plotted against the number of transferred nucleons  $n$ .

### 3. Reactions for larger number of transferred particles

The variation of the  $Q^m$  with the  $E_{\text{lab}}$  and  $n$  was discussed above (Fig. 7).

For reactions involving  $n$  larger than 4–5, the residual energy of the particle traveling in the nuclear matter, probably at its diffuse rim, will become insufficient to dissipate energy at the same rate  $\alpha_{\text{eff}}$ , hence the linearity (3) breaks down and  $Q_{\text{eff}}^m$  saturates with respect to  $n$  (Figs. 8 and 9). However, this saturation may be due to different reaction mechanisms such as transfer in cluster, breakup of the projectile, sequential decay and/or a compound nuclear reaction. For the largest  $n$ , i.e.,  $n=10$  with  $b=^4\text{He}$  in the present case,  $Q_{\text{eff}}^m \approx V_C^i - E_i$ , irrespective of the incident variables. This is a necessary but not a sufficient condition that the reaction proceed via a compound nucleus.<sup>21</sup> The angular distribution of the emitted  $\alpha$  particles are peaked in the forward direction. The possibility of breakup of the projectile,  $a \rightarrow b + c$ , where  $c$  is an unobserved particle, cannot be ruled out, merely on the basis of kinematic consideration for  $n \geq 4$ .<sup>12</sup>

## IV. CONCLUSION

The spectrum of outgoing particles,  $b$ , for multinucleon transfer reactions  $A(a, b)$ , induced by heavy ions of energy much higher than the Coulomb barrier were investigated. The discussion has been limited to the higher-energy part of the spectrum for  $M_b < M_a$ , when two components were observed.

Throughout a wide range of  $E_i$  and  $A + a$ , the simple linear relation (3) between the most probable effective  $Q$  value,  $Q_{\text{eff}}^m$ , vs  $n$ , the number of transferred nucleons, was obtained for  $n \leq 4-5$ . It was found that a constant amount of energy  $\alpha_{\text{eff}}$ , which is about one-tenth of the energy available at the barrier  $E_i - V_C^i$ , is lost per nucleon transferred.

The key factors which govern the reaction are the energy loss of the scattering particle in the diffuse rim of the nuclear matter and the level density of the residual nucleus. The occurrence of reactions at the very diffuse rim is deduced, in  $^{52,53}\text{Cr} + ^{14}\text{N}$  reactions, from the very weak dependence of  $Q^m$  and  $\theta_{\text{lab}}$  and a constant value of  $\beta$  in Eq. (2). The values of  $Q_{\text{eff}}^m$  are independent of the  $N$  and  $Z$  of individual adjacent target nuclei and hence of their nuclear structure. For reactions of  $^{14}\text{N} + \text{Cr}$ , even  $Q^m$  depends only on  $n$  [Eq. (2)], irrespective of neutron and proton transfer.

The ratio of the most probable final velocity to the incident velocity  $v_f^m/v_i$  is about unity for  $n=1$  and decreases as  $n$  increases.

For  $n > 4-5$ , the linear relation breaks down and the role of other reaction mechanisms becomes more important.

The energy and mass regions studied here play the role of a "bridge" between the reactions of very heavy nuclei, dominated by deep inelastic processes<sup>2,22</sup> and those between lighter heavy ions, which reveal many selective peaks.<sup>23</sup>

#### ACKNOWLEDGMENT

The authors would like to express their thanks to the cyclotron crew of IPCR. They wish to thank Dr. D. M. Brink, Dr. D. K. Scott, Dr. R. H. Siemssen, Dr. P. J. Siemens, Dr. M. Lefort, Dr. M. Ishihara, and Dr. T. Kohmura for their valuable discussions.

\*Institute of Physics, University of Tsukuba, Ibaraki, Japan and Department of Physics, Tokyo University of Education, Otsuka, Bunkyo-ku, Tokyo.

†Department of Physics, University of Tokyo, Bunkyo-ku, Tokyo.

<sup>1</sup>(a) A. G. Artukh, G. F. Gridnev, V. L. Mekheev, V. V. Volkov and J. Wilczyński, Nucl. Phys. **A168**, 321 (1971); (b) **A211**, 299 (1973).

<sup>2</sup>A. G. Artukh, G. F. Gridnev, V. L. Mikheev, V. V. Volkov and J. Wilczyński, Nucl. Phys. **A215**, 91 (1973).

<sup>3</sup>(a) T. Mikumo, I. Kohno, K. Katori, T. Motobayashi, S. Nakajima, M. Yoshie, and H. Kamitsubo, in *Proceedings of the International Conference on Reactions between Complex Nuclei, Nashville, 1974* (North-Holland, Amsterdam, 1974), Vol. 1, p. 64; (b) Proceedings of the INS-IPCR Symposium on Cluster Structure of Nuclei and Transfer Reactions Induced by Heavy Ions, Tokyo [IPCR Cyclotron Progress Report Suppl. 4, 1975, p. 617]; (c) H. Kamitsubo, *ibid.*, p. 623; (d) H. Kamitsubo, M. Yoshie, I. Kohno, S. Nakajima, I. Yamane, and T. Mikumo, Symposium on Heavy-Ion Transfer Reactions [Argonne Physics Division Informal Report No. PHY-1973 B, March 1973 (unpublished), Vol. II, pp. 549, 573].

<sup>4</sup>P. J. A. Buttle and L. J. B. Goldfarb, Nucl. Phys. **A176**, 299 (1972).

<sup>5</sup>J. P. Schiffer, H. F. Körner, R. H. Siemssen, K. W. Jones and A. Schwarzschild, Phys. Lett. **44B**, 47 (1973).

<sup>6</sup>W. von Oertzen, in Symposium on Heavy-Ion Transfer Reactions [Argonne Physics Division Informal Report No. PHY-1973 B, March 1973 (unpublished), Vol. II., p. 675]; *Lecture Notes in Physics* (Springer-Verlag, Berlin, 1973), Vol. 23, p. 267.

<sup>7</sup>D. M. Brink, Phys. Lett. **40B**, 37 (1972).

<sup>8</sup>P. J. Siemens, J. P. Bondorf, D. H. E. Gross, and

F. Dickmann, Phys. Lett. **36B**, 24 (1971).

<sup>9</sup>J. Wilczyński, Phys. Lett. **47B**, 124 (1973).

<sup>10</sup>Y. Miyazawa, T. Tonuma, and I. Kohno, Jpn. J. Appl. Phys. **9**, 532 (1970).

<sup>11</sup>I. Kohno, S. Nakajima, T. Tonuma, and M. Odera, J. Phys. Soc. Jpn. **30**, 910 (1970).

<sup>12</sup>I. Kohno, K. Katori, T. Mikumo, T. Motobayashi, S. Nakajima, M. Yoshie, and H. Kamitsubo (unpublished).

<sup>13</sup>M. Yoshie and I. Kohno, Sci. Papers Inst. Phys. Chem. Res. **69**, No. 3 (1975); (unpublished).

<sup>14</sup>J. P. Bondorf, F. Dickmann, D. H. E. Gross, and P. J. Siemens, J. Phys. (Paris) **32**, C6-145 (1971).

<sup>15</sup>L. G. Moretto, S. K. Kataria, R. C. Jared, R. Schmitt, and S. G. Thompson, Nucl. Phys. **A255**, 491 (1975).

<sup>16</sup>J. Wilczyński, K. Siwek-Wilczyńska, J. S. Larsen, J. C. Acquadro, and P. R. Christensen, Nucl. Phys. **244**, 147 (1975).

<sup>17</sup>W. Henning *et al.*, Heidelberg Spring Meeting Verhandl. DPG (VI) **8**, 23 (1973), cited by H. Körner, Symposium on Heavy-Ion Transfer Reactions [Argonne Physics Division Informal Report No. PHY-1973 B, March 1973 (unpublished), Vol. I, p. 9].

<sup>18</sup>V. V. Volkov, F. Gridnev, G. N. Zorin, and L. P. Chel'nikov, Nucl. Phys. **A126**, 1 (1969).

<sup>19</sup>J. P. Bondorf and W. Nörenberg, Phys. Lett. **44B**, 487 (1973).

<sup>20</sup>J. Galin, D. Guerreau, M. Lefort, J. Péter, X. Tarrago, and R. Basile, Nucl. Phys. **A159**, 461 (1970).

<sup>21</sup>D. M. Brink (private communications).

<sup>22</sup>F. Hanappe, M. Lefort, C. Ngo, J. Péter, and B. Tam-in, Phys. Rev. Lett. **32**, 738 (1974).

<sup>23</sup>N. Anyas-Weiss, J. Cornell, P. Fisher, P. N. Hudson, A. Mecha-Rocha, D. J. Millener, A. D. Panagiotou, D. K. Scott, D. Strottman, D. K. Brink, B. Buck, P. J. Ellis, and T. England, Phys. Rep. **12C**, 201 (1974).